The Journal of Experimental Biology 216, 4580-4589

doi:10.1242/jeb.094516

RESEARCH ARTICLE

Proteomic response of marine invertebrate larvae to ocean acidification and hypoxia during metamorphosis and calcification

Joy Mukherjee[1], Kelvin K. W. Wong[1], Kondethimmanahalli H. Chandramouli[2], Pei-Yuan Qian[2], Priscilla T. Y. Leung[1], Rudolf S. S. Wu[3] and Vengatesen Thiyagarajan[1,*]

[1]The Swire Institute of Marine Science and School of Biological Sciences, The University of Hong Kong, Hong Kong SAR, [2]Division of Life Science, The Hong Kong University of Science and Technology, Hong Kong SAR and [3]Centre for Marine Environmental Research and Innovative Technology, School of Biological Science, The University of Hong Kong, Hong Kong SAR

*Author for correspondence (rajan@hku.hk)

SUMMARY

Calcifying marine invertebrates with complex life cycles are particularly at risk to climate changes as they undergo an abrupt ontogenetic shift during larval metamorphosis. Although our understanding of the larval response to climate changes is rapidly advancing, the proteome plasticity involved in a compensatory response to climate change is still unknown. In this study, we investigated the proteomic response of metamorphosing larvae of the tubeworm *Hydroides elegans*, challenged with two climate change stressors, ocean acidification (OA; pH 7.6) and hypoxia (HYP; 2.8 mg O_2 l^{-1}), and with both combined. Using a two-dimensional gel electrophoresis (2-DE)-based approach coupled with mass spectrometry, we found that climate change stressors did not affect metamorphosis except under OA, but altered the larval proteome and phosphorylation status. Metabolism and various stress and calcification-related proteins were downregulated in response to OA. In OA and HYP combined, HYP restored the expression of the calcification-related proteins to the control levels. We speculate that mild HYP stress could compensate for the negative effects of OA. This study also discusses the potential functions of selected proteins that might play important roles in larval acclimation and adaption to climate change.

Supplementary material available online at http://jeb.biologists.org/lookup/suppl/doi:10.1242/jeb.094516/-/DC1

Key words: environmental proteomics, hypoxia, larval metamorphosis, ocean acidification.

Received 28 July 2013; Accepted 2 September 2013

INTRODUCTION

The majority of marine invertebrates, including biofouling species such as barnacles and tubeworms, have complex life cycles that include an intricately controlled metamorphic process involving the transformation from swimming (planktonic) larvae to sessile (attached or benthic) adults in a few minutes (Hadfield, 2000; Qian, 1999). This transformation is one of the most challenging processes in the life history of an organism, requiring the simultaneous performance of multiple tasks. The tasks involve choosing a new habitat to settle on, switching the molecular machinery to adapt to sessile life, and building a protective calcareous shell or tube by controlled calcification (Thiyagarajan, 2010). In recent years, rapid developments in environmental molecular biology and chemical ecology have shed light on some key questions: how do larvae choose where to settle (Huang et al., 2012); what triggers the transformation from planktonic to benthic life (Dreanno et al., 2006); and what genes are involved in such transformations (Hayward et al., 2011)? Despite the rapid increase in proteomics studies on non-model (where the genome has not been completely sequenced) species (Diz and Skibinski, 2007; McDonagh and Sheehan, 2006; Nunn and Timperman, 2007; Tomanek, 2006; Tomanek, 2011), proteins and their post-translational modifications (PTMs) involved in larval metamorphosis and calcification are still largely unknown (Chandramouli et al., 2011).

With rising anthropogenic CO_2-driven changes to the global climate system, larvae now face unprecedented threats from multiple stressors associated with climate change (Byrne, 2011; Dupont and Thorndyke, 2009; Hofmann et al., 2010). For instance, increasing CO_2 causes ocean acidification (OA), resulting in the depletion of a significant portion of carbonate ions, which can disrupt larval calcification (Feely et al., 2004). Physiological mechanisms that regulate internal pH homeostasis and calcification become more expensive or impaired under OA (Pörtner, 2008). Marine species are unlikely to adapt in sufficient time to these rapid changes in seawater chemistry that are predicted to occur in <100 years (Sabine et al., 2004; Sunday et al., 2011). Calcifying marine organisms undergo an abrupt ontogenetic shift in their habitat and environmental conditions as the free-swimming larvae settle, during which time they metamorphose into adults (Hadfield, 2000) and form their shell or tube through calcification (Vinn et al., 2008). Diverting their finite energy resources to cope with the climatic changes would disrupt these energy-expensive processes. The larval shells or tubes are made of the $CaCO_3$ mineral aragonite, which is highly soluble in low pH seawater (Chan et al., 2012). Even a slight decrease in pH (from control pH 8.1 to 7.7) delays or hinders the calcification processes in the larvae of metamorphosing tubeworms (Lane et al., 2013). The survival of such animals is highly threatened unless they have a sufficient physiological compensatory response or possess the capacity to acclimate by altering their global gene and/or protein expression pattern.

Concurrently, anthropogenic activities such as the discharge of excessive nutrients, sewage and agricultural fertilizers are causing

coastal waters to become increasingly nutrient rich (Howarth et al., 2011). The nutrient overload increases algal production and this excessively produced biomass eventually decomposes, resulting in dead zones, areas of hypoxia that have become deprived of dissolved oxygen (Ekau et al., 2010; Rabalais et al., 2010). Coastal hypoxia events are expected to increase as a consequence of regional and global climate change (Gilbert et al., 2010; Peña et al., 2010). Hypoxia has been shown to be responsible for triggering mortality events that deplete marine organisms including tubeworms (Leung et al., 2013; Lo et al., 2011; Wu, 2009). Furthermore, OA effects could be exacerbated under hypoxia as more CO_2 is released as the oxygen is consumed (Melzner et al., 2013). The ability of larvae to successfully metamorphose and build their calcareous tubes is likely to be compromised as a direct consequence of the combined effect of OA and hypoxia. It is not known what complex proteome-wide changes occur in response to climate change during larval metamorphosis. Therefore, it is important to study the global proteome-level changes (molecular proteome plasticity) in larvae to understand how they respond to overcome these climate change threats.

Recently, proteomics analyses have been recognized as promising molecular tools that can be used to study larval development (Thiyagarajan and Qian, 2008), metamorphosis (Mok et al., 2009), perception of chemical signals (Thiyagarajan et al., 2009) and response to various environmental changes including OA (Dineshram et al., 2012; Wong et al., 2011). Although two-dimensional gel electrophoresis (2-DE)-based proteomics is widely used in larval biology research, it has been used in only a few climate change studies (Thiyagarajan, 2010; Tomanek, 2011). For example, a marked reduction of expressed proteins was observed in oyster larvae exposed to OA (Dineshram et al., 2013; Dineshram et al., 2012). In another study, several key energy-related proteins were differentially regulated in barnacle larvae under OA (Wong et al., 2011). Taken together, these previous studies suggest that larvae of certain marine invertebrate species can differentially regulate the expression of calcification and/or metabolism-related proteins as a compensatory response to OA. We propose that the larval proteome changes would underlie the negative effects of OA, including reduced calcification rate and metabolic depression, which are commonly observed in other species (Dupont and Thorndyke, 2009; Talmage and Gobler, 2011). Similarly, proteome changes could be present in response to hypoxia conditions, which is known to trigger metabolic depression through reduction of the aerobic metabolic rate and the critical oxygen tension required for aerobic metabolism (Seibel, 2011). In this study, we hypothesize that larval acclimation and/or short-term adaption to climate change occurs at the proteome level, specifically, differential changes in proteins associated with calcification, energy metabolism and stress tolerance. To test these hypotheses, we investigated the potential molecular repertoire (i.e. proteome plasticity) of the larval response of the tubeworm *Hydroides elegans* to the two individual stressors or combined stressors using a 2-DE proteomics approach. The protein expression signatures involved in acclimation of the larval physiological tolerable limits during metamorphosis was analyzed.

MATERIALS AND METHODS

Test organism and larval culture

The tubeworm *Hydroides elegans* (Haswell 1883) was selected as the model because: (1) they can be cultured year-round in the laboratory because of their short life cycle (Qian, 1999); (2) they have morphologically distinct developmental stages during metamorphosis (supplementary material Fig. S1); (3) their transcriptome and expressed sequence tag (EST) sequences are available for use in proteomic studies (P.-Y.Q., unpublished data); and (4) this species has been declared as model for larval research, including OA studies (Lane et al., 2013; Nedved and Hadfield, 2009). Tubeworms were collected from floating objects from a fish farm in Hong Kong (22°19′N, 114°16′E) and then conditioned in the laboratory for several days under ambient conditions (pH 8.1, dissolved oxygen 6.4 mg O_2 l^{-1}, salinity 33‰ and 24°C). Tubeworms in 0.22 μm filtered seawater (FSW) were prepared for spawning by breaking their tubes (Pechenik et al., 2007). For fertilization, gametes from approximately 100 females were mixed with sperm from approximately 25 males in FSW (Pechenik and Qian, 1998). After 1 h post-fertilization, embryos were isolated for use in the experiments below.

Climate change conditions and experimental design

The individual and combined effects of two climate change variables, OA and hypoxia (HYP), on the proteome of tubeworm larvae were accessed. OA treatments had two levels: an ambient pH of 8.1 and a low pH of 7.6. The low pH value is representative of the projected annual average pH value for the years 2100 and 2300 (Caldeira and Wickett, 2005). HYP treatments also had two levels: an ambient oxygen level (4.8±0.3 mg O_2 l^{-1}) and a moderately low oxygen level (2.8±0.2 mg O_2 l^{-1}). Environments with dissolved oxygen (DO) levels of 2.8±0.2 mg O_2 l^{-1} or below are considered to be hypoxic as defined in the literature (Diaz and Rosenberg, 1995). We assessed the effect of OA and HYP individually and combined (OA×HYP), comparing the treatments with the control at ambient pH and ambient DO levels. Three biologically independent replicates were analyzed for each condition.

The OA levels were achieved by bubbling CO_2-enriched air into the tanks at rates sufficient to achieve the desired low-pH level according to the European Project on Ocean Acidification standard procedure (Riebesell et al., 2010). The CO_2-enriched air was prepared by adjusting the flow rate of air and CO_2 using dual (air and CO_2) variable area flow meter/controllers (Cole-Parmer, Chicago, IL, USA) (Lane et al., 2013). The pH was measured twice a day throughout the experimental period using a pH meter (NBS scale; Mettler-Toledo, Columbus, OH, USA). Total alkalinity was measured using an Apollo SciTech AC-A2 Alkalinity Titrator (Bogart, GA, USA), calibrated using seawater reference material provided by A. G. Dickson (Scripps Institution of Oceanography, La Jolla, CA, USA). The carbonate chemistry of each tank was calculated using the CO2SYS program (Lewis and Wallace, 1998). The required DO level was maintained by constantly bubbling air mixed with appropriate amounts of ultrapure nitrogen (N_2) gas (Leung et al., 2013). The N_2-enriched air was prepared by adjusting the flow rate of air and N_2 using dual variable area flow meter/controllers (Cole-Parmer). The DO level was measured at least twice a day using a calibrated (by Winkler titration) Orion 5-Star Plus Meter (Thermo Fisher Scientific, West Palm Beach, FL, USA). The OA×HYP treatment levels were maintained by bubbling air mixed with appropriate amounts of N_2 and CO_2.

Embryos (10 embryos ml^{-1}) were added into each of the 12 (four treatment conditions × three replicates) culture/treatment tanks containing 4 liters of FSW. Culture tanks were maintained under a florescent room light at constant temperature (25°C) and salinity (32 to 34‰). Every 24 h, any undeveloped embryos or dead larvae were sieved out, the culture medium was replenished, and concentrated algal (*Isochrysis galbana*) suspensions (~10^5 cells ml^{-1}) were added as the food source (Qian, 1999). The treatment pH, DO levels, temperature and salinity were closely monitored and were maintained at relatively constant levels throughout the experiment.

Algal photosynthesis or respiration had minimal influence on the treatment levels (supplementary material Fig. S2). The larvae reached competency to settle and metamorphose into juvenile tubeworms (supplementary material Fig. S1) at approximately 4 to 5 days. They were triggered to settle and form calcified protective tubes on 1 liter glass beaker walls using an artificial settlement inducer, 3-isobutyl-1-methylxanthine (IBMX; 10^{-4} mol l^{-1}) (Qian and Pechenik, 1998). After 24 h of incubation, the newly metamorphosed juveniles were rinsed with distilled Milli-Q water and carefully scraped off the glass beaker wall. They were immediately frozen in 2-DE lysis buffer (7 mol l^{-1} urea, 2 mol l^{-1} thiourea, 4% CHAPS, 40 mmol l^{-1} dithiothreitol and 2% Bio-Lyte 3/10 ampholyte) with protease inhibitor and stored at −70°C. The percentage of larval metamorphosis and calcification was determined by subtracting the number of swimming larvae from the total number of larvae used in the settlement assay.

Multiplex staining and analysis of 2-DE gels

A standardised 2-DE protocol optimized for tubeworm larval proteome analysis was used (Zhang et al., 2010a). Proteins were extracted by sonication (Apollo Ultrasonics, York, UK) followed by centrifugation at 14,000 ***g*** for 20 min at 4°C. The supernatant was collected and stored at −70°C until use. The protein concentration in the supernatant was determined using the modified Bradford method (Ramagli, 1999). Exactly 150 µg of proteins was applied to narrow-range (pH 3–6, liner gradient) 11 cm immobilized pH gradient (IPG) strips (Bio-Rad Laboratories, Hercules, CA, USA) in rehydration buffer (three biological replicates were analyzed). The proteins on the IPG strips were separated according to their isoelectric point using a Protean IEF Cell (Bio-Rad). For the second dimension, the equilibrated IPG strips were loaded on 12.5% SDS-PAGE gels and run at 200 V. The gels were stained with Pro-Q Diamond phosphoprotein stain (Pro-Q DPS; Molecular Probes, Life Technologies, Grand Island, NY, USA) followed by Sypro-Ruby total protein stain (Molecular Probes), and finally with Blue Silver stain (modified Neuhoff's colloidal Coomassie Brilliant Blue G-250; Sigma-Aldrich, St Louis, MO, USA) to visualize the protein spots (Candiano et al., 2004). The gels were stained with Sypro-Ruby prior to staining with Blue Silver to sensitize the gels for better linearity, which gives considerably higher sensitivity than staining with only Blue Silver (Yang et al., 2011).

Proteome analysis

Proteome analysis was carried out using Progenesis SameSpots v3.0 (Nonlinear Dynamics, Newcastle upon Tyne, UK) and PDQuest (Version 8.0; Bio-Rad). Images were aligned using prominent spots as a landmark and all subsequent gels were comparatively analyzed. The spots identified by the software as differentially expressed were checked manually to confirm the software analyses. The Progenesis software models the proteins mathematically using an alignment-based approach. The PDQuest software models the proteins mathematically as a 3-D Gaussian distribution and determines the maximum absorption after correction and background subtraction. Protein spot intensities were normalized according to the total intensity of all spots in each gel and then statistically analyzed using one-way ANOVA and fold-change methods. Protein spots displaying a statistical difference greater than 1.5-fold between the experimental treatments were considered as differentially expressed. For the total proteins, three replicates per treatment were used. For the Pro-Q Diamond phosphoprotein stain, gel spots on the third replicates for controls and OA were over-stained, and only two replicates of these were used for analysis.

The protein spot intensities were subjected to multivariate statistical analysis by principal component analysis (PCA) using PRIMER 6 software (PRIMER-E, Plymouth, UK). The multivariate analysis was based on the Euclidean distance matrix calculated from log-transformed protein spot intensity data, with pair-wise tests conducted between groups. PCA is one of the most commonly used techniques for an in-depth search of predominant proteomic patterns in a large dataset (Halko et al., 2011).

Identification of differentially expressed proteins

From the 2-DE, 13 abundant and differentially expressed proteins were excised from the gels and destained with 50% methanol in 50 mmol l^{-1} NH_4HCO_3. The gels were rinsed with MilliQ water, and then washed in 10 mmol l^{-1} NH_4HCO_3 and 100% acetonitrile (ACN). The gel plugs were rehydrated with 20 µl of 12.5 ng μl^{-1} trypsin (Promega, Madison, WI, USA) in 10 mmol l^{-1} NH_4HCO_3. After incubation for 16 h at 37°C, the peptides were extracted using 5% formic acid (FA)/50% ACN and then washed with 100% ACN. After drying in a volume concentrator, the peptides were resuspended in 0.1% FA, and purified using µC-18 Ziptips (Millipore, Bedford, MA, USA). The desalted peptides were then mixed in a 1:1 ratio with 10 mmol l^{-1} CHCA matrix dissolved in 0.1% FA/50% ACN (Shevchenko et al., 2007).

Peptides were examined using a 4800 MALDI-TOF/TOF analyser running the 4000 Series Explorer version 3.5.28193 software (both Applied Biosystems, Foster City, CA, USA). Mass spectra (MS) were acquired in the reflector positive ion mode with 500 shots per spot. Before each job run, the MS and the MS/MS were calibrated using the six-peptide calibration standard, 4700 Cal-Mix (Applied Biosystems), which was spotted across 13 locations on the MALDI target plate. The MS were recorded in the mass range from 900 to 4000 Da. The five most intense precursor ion peaks from peptide mass fingerprinting (PMF) were further subjected to post-source decay fragmentation (collision-induced dissociation was off, 2 keV collision energy) to determine the peptide sequence. A combined PMF and MS/MS search was performed using GPS Explorer algorithm version 3.6 (Applied Biosystems) against the non-redundant NCBInr database using the in-house MASCOT search engine version 2.2 (containing

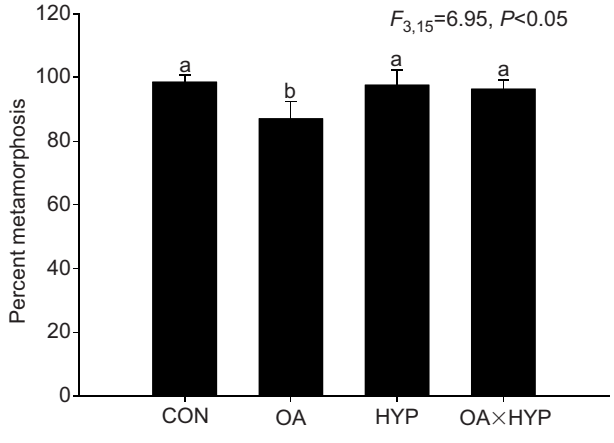

Fig. 1. The effects of ocean acidification (OA) and hypoxia (HYP) individually and combined (OA×HYP) on the metamorphosis and calcification of the *Hydroides elegans* larvae. Each bar represents the mean ± s.d. of three replicates. Mean values were tested for significant differences using one-way ANOVA. Data that are significantly different (α=0.05, Tukey's test) are indicated by different letters above the bars. CON, control.

15,322,545 sequences; Matrix Science, Boston, MA, USA). The following parameters were used in all MASCOT searches: monoisotopic peptide masses, mass tolerance settings of ±75 ppm for PMF and ±0.2 Da for the MS/MS, tolerance of one missed cleavage, carbamidomethylation of cysteine as the fixed modification, oxidation of methionine as the variable modification, and taxonomy filter restricted to 'other Metazoa' (containing 933,410 sequences). The criteria for protein identification were based on the probability score of each search result. Significant matches had scores greater than the minimum threshold set by MASCOT (with $P<0.05$) (Carpentier et al., 2008).

Western blot analysis

Western blot analysis was performed to confirm the differential expression of a key target protein, tubulin (Chandramouli et al., 2012). Protein (15 µg) from the control and the other treatment groups were run on 1-D 12.5% SDS-PAGE and transferred onto nitrocellulose membrane. The membrane was blocked using 5% (w/v) non-fat dry milk in TBS buffer containing 0.1% Tween-20. The membrane was incubated with primary tubulin antibody (Cell Signaling, Danvers, MA, USA) and then with anti-rabbit secondary antibody (GE Healthcare, Barrington, IL, USA). The blots were detected using an electrochemiluminescence kit (Millipore, Billerica,

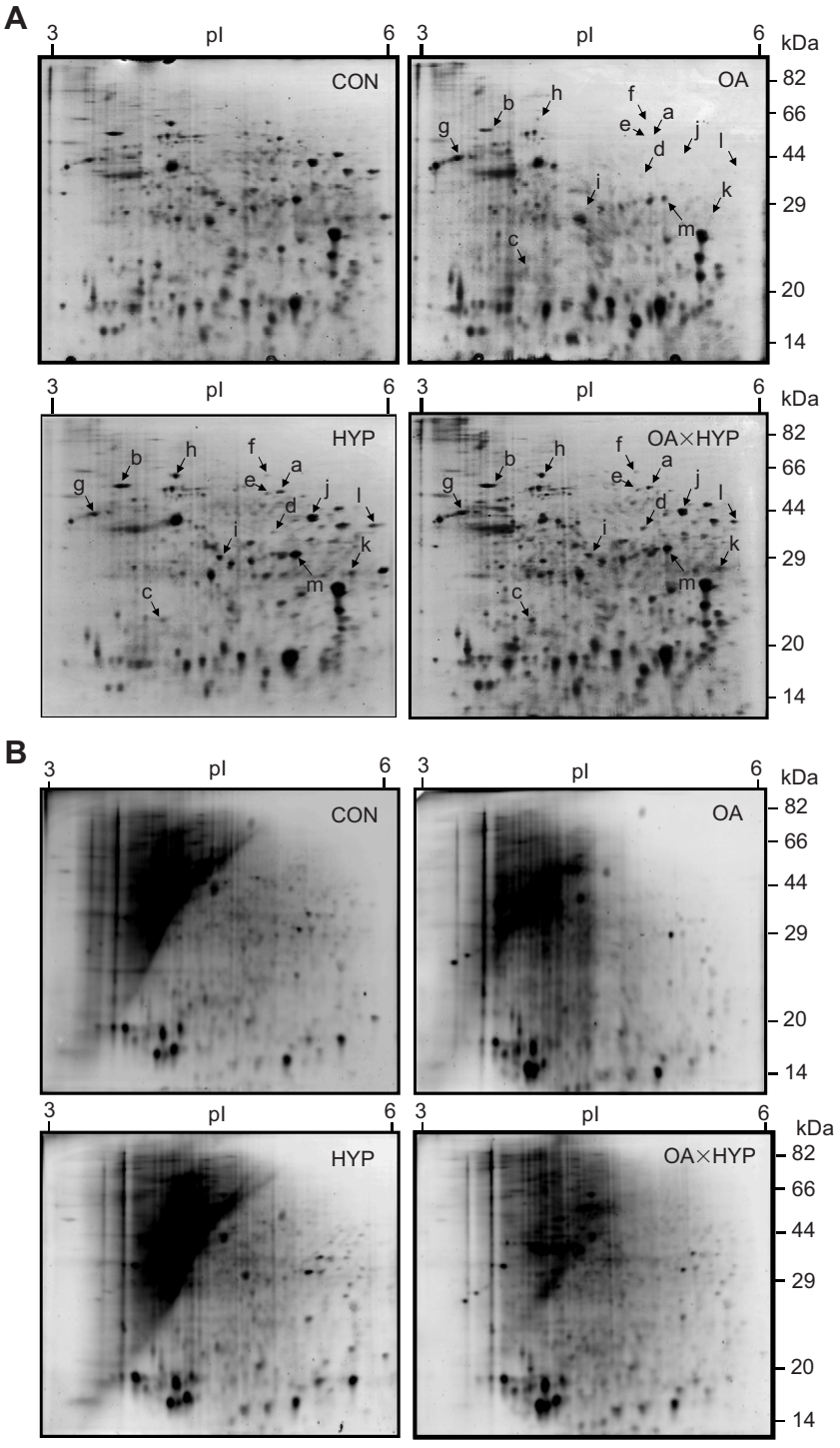

Fig. 2. Gel images of the total proteins (A) and phosphoproteins (B) visualized in the newly metamorphosed *Hydroides elegans* larvae (or juveniles) in the control (CON), ocean acidification (OA), hypoxia (HYP) and combined OA×HYP groups. The proteins spots that are differentially expressed (indicated by an arrow) were identified using MALDI TOF/TOF and are detailed in Table 1. pI, isoelectric point.

MA, USA) and images were scanned using a GS-800 calibrated densitometer (Bio-Rad).

RESULTS AND DISCUSSION

Larval metamorphosis and calcification

Treatment conditions were maintained at relatively stable levels over the course of the experiments (supplementary material Fig. S2B). Notably, the carbonate system attributes such as pH and $CaCO_3$ mineral saturation levels were maintained at expected treatment levels (supplementary material Table S1). The percentage of larval metamorphosis and calcification induced by the artificial inducer (IMBX) was significantly lower under OA compared with the other two treatment conditions and the control (Fig. 1). The newly metamorphosed larvae seemed to tolerate the combined effect of climate change stressors, HYP and OA, during metamorphosis and calcification. Possibly, hypoxia had a compensatory effect when combined with OA, which was contrary to our hypothesis that HYP would adversely affect metamorphic success and would further exaggerate the negative effects of OA. As pH levels are expected to be lower than 7.5 under hypoxic conditions, future studies should look into the potential interactive effects of HYP and OA at pH<7.5.

Organisms that live under elevated or variable CO_2 environments such as hydrothermal vents, tide pools and near CO_2 vents have greater capacity for buffering internal fluids, ion exchange and CO_2 transport (Pörtner, 2008). Tubeworm larvae that build the pH-sensitive aragonite tubes appear to be incapable of coping with elevated CO_2, resulting in significantly decreased metamorphosis and calcification at pH 7.6. Nevertheless, the physiological mechanisms adapted by tubeworm larvae to negate the negative effects of elevated CO_2 (OA) under HYP remain unclear. Marine surfaces with densely populated microbial biofilms and biofouling communities often experience HYP (Lindgren et al., 2009), but tubeworm larvae still tend to metamorphose and form their calcified tubes (Hadfield, 2011). Therefore, tubeworm larvae may have physiological mechanisms to acclimate to HYP. Under HYP, animals tend to develop greater pH sensitivity to release more metabolic oxygen to cope with high oxygen demand or produce high-affinity respiratory proteins (Fabry et al., 2008). Such elevated HYP-adaptive physiological mechanisms may have played a key role in negating the OA effect.

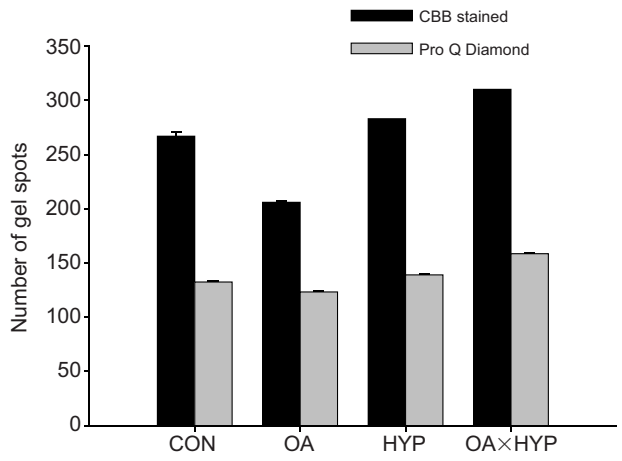

Fig. 3. Number of total protein (A) and phosphoprotein (B) spots identified using PDQuest software in the control (CON), ocean acidification (OA), hypoxia (HYP) and combined OA×HYP groups. Each bar represents the mean ± s.d. of three biological replicates. CBB, Coomassie Brilliant Blue.

Proteome response

Representative total proteome and phosphoproteome maps of the newly metamorphosed larvae or juveniles in the control, OA, HYP and OA×HYP treatment groups are shown in Fig. 2A and 2B, respectively. Total larval proteome maps obtained from three different biologically independent samples showed reproducible protein patterns in both total protein and phosphoprotein stained gels (supplementary material Fig. S3). Under OA, the average number of Coomassie Brilliant Blue stained total proteins decreased considerably to 206 spots. However, we observed a slight increase in protein expression under HYP (average 283 spots; Fig. 3). The number of detectable total proteins in tubeworms in the OA×HYP treatment group increased to 310 spots, which was higher than in the control group. Interestingly, the percentage of phosphorylated proteins showed an opposite trend to the total protein results (Fig. 3). More than 60% of proteins were found to be phosphorylated in the OA group, whereas ~50% of proteins were phosphorylated in the other treatments. Specifically, the percentage of phosphorylated proteins was much higher in the OA group compared with the

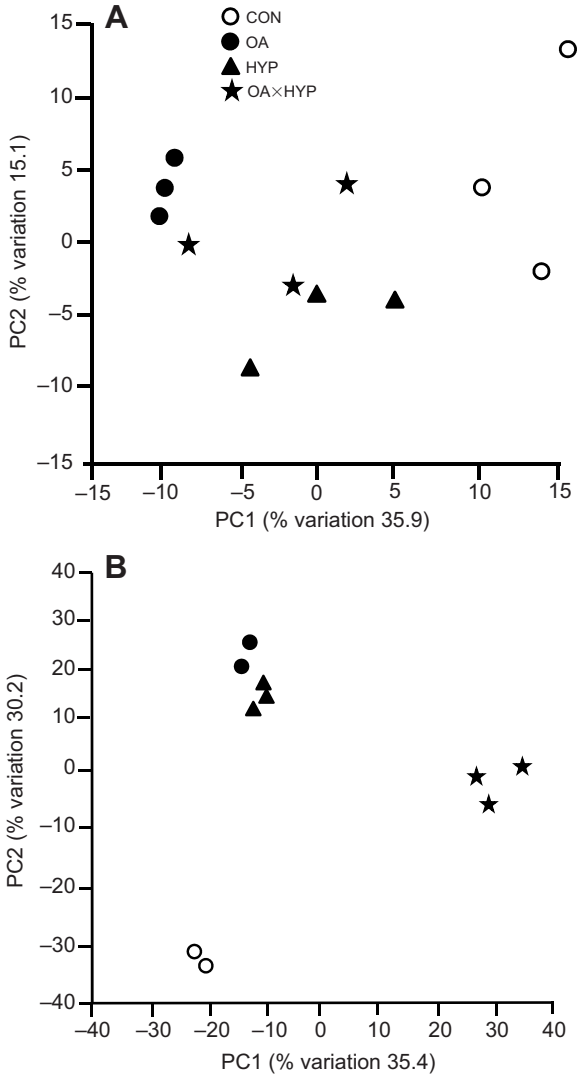

Fig. 4. Multivariate statistical analysis results of the 2-DE protein expression profiles in *Hydroides elegans* are shown as a principal component (PC) analysis plot illustrating the global difference of the (A) total proteins and (B) phosphoproteins identified in the control (CON), ocean acidification (OA), hypoxia (HYP) and combined OA×HYP groups.

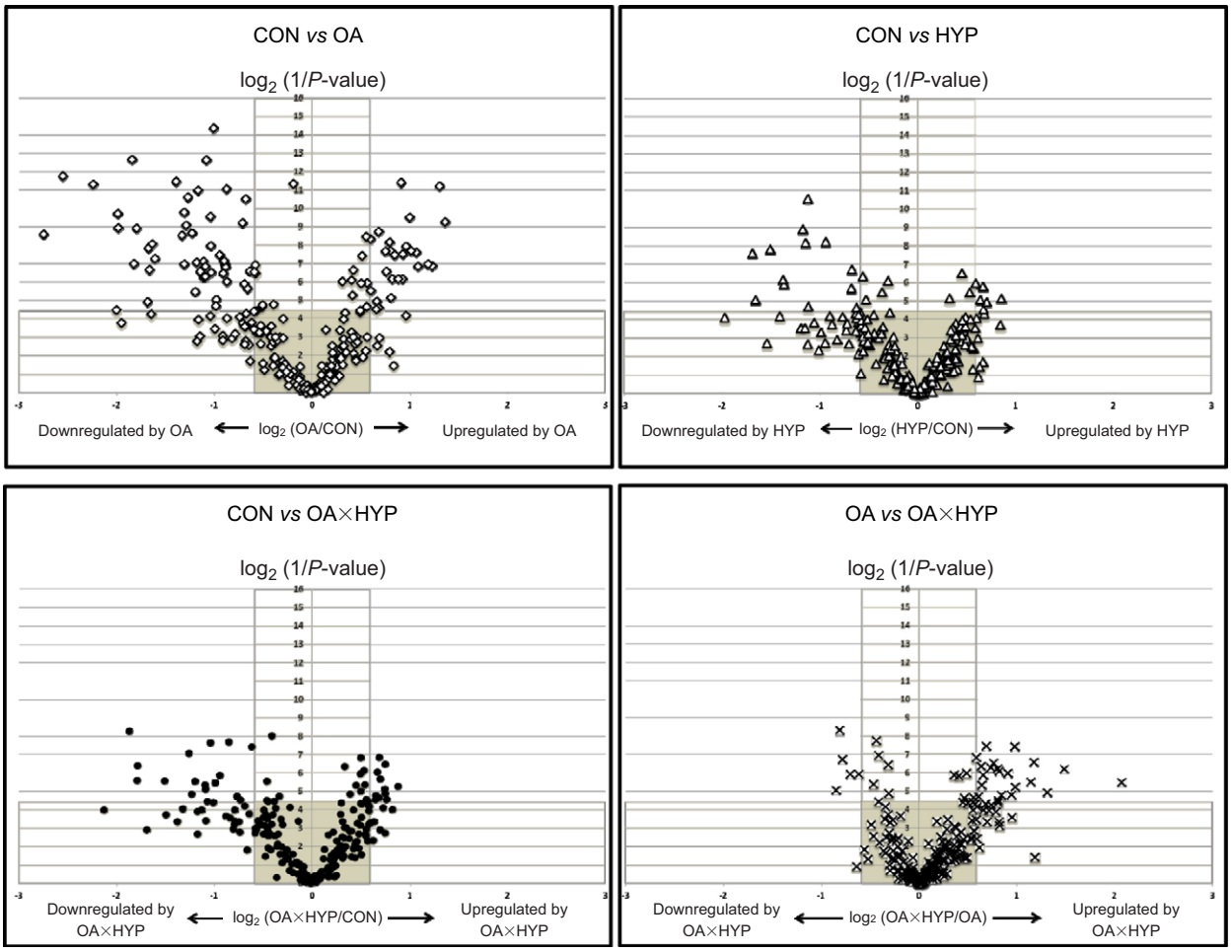

Fig. 5. Volcano plots of the 2-DE data set showing the relationship between the magnitude of expressed proteins in the control (CON) and ocean acidification (OA) groups, between CON and hypoxia (HYP), between CON and OA×HYP, and between OA and OA×HYP. The 2-DE (total protein) spot intensity data were obtained using Progenesis SameSpots analysis software. The protein spots lying outside the shaded area in the plot indicate either upregulation or downregulation.

OA×HYP group. This was contrary to our hypothesis that the combined effects of OA and HYP would result in more PTM-regulated proteins than OA alone.

In the PCA, PC1 showed that the OA group was separated furthest away from the other three treatment groups (Fig. 4A). This indicates that the tubeworm larvae reared under OA conditions exhibit a substantially distinct proteomic profile compared with their counterparts in the control, HYP or OA×HYP groups. PC2 further separated the control and HYP groups, and the OA×HYP group lay in between the two. On the PCA plot, the HYP and OA×HYP groups were closely related, suggesting that that HYP exerted a compensatory effect on OA, leading to a shift in proteome dynamics of the tubeworm larvae compared with OA alone. The control and OA samples formed two distinct groups, illustrating a dramatic change in the juvenile proteome in response to OA. Moreover, the OA and the OA×HYP groups were also clustered into different groups, illustrating that HYP had a compensatory effect on OA, so their expressions are different.

From the PCA plot (Fig. 4B), PC1 showed that the phosphoproteome of the control group was the furthest from the other three groups, and PC2 showed that the OA×HYP group was separated from the HYP group and the OA group. The observation of opposite changes in phosphoprotein distribution across the two-dimensional space suggests that the tubeworm larvae might employ a different strategy for regulating cellular functions in response to climate changes. Previous studies have shown that marine organisms can reprioritize metabolic processes through selective changes in total proteome and/or phosphoproteome (Wong et al., 2011; Zhang et al., 2010a; Zhang et al., 2010b).

Larval proteome plasticity

Only a few visible signs of developmental changes and phenotypic adjustments were apparent in metamorphosing and calcifying larvae in response to climate change stressors, but more intrinsic differences were observed in their respective protein expression signatures (Fig. 2). There seems be a high degree of proteome plasticity in larval tubeworms in response to climate change. One of the most prominent changes was the widespread downregulation or under-expression of a multitude of proteins in the OA group, which was in agreement with our previous finding of nearly 50% under-expression of the total resolved proteins in response to a similar level of OA in the oyster larvae (Dineshram et al., 2012). Correspondingly, our hypoxia results were similar to those found in hypoxia-exposed oyster adults, where only a minor proportion of transcripts showed hypoxia-associated changes that ranged from slightly differentially expressed to a few that were strongly

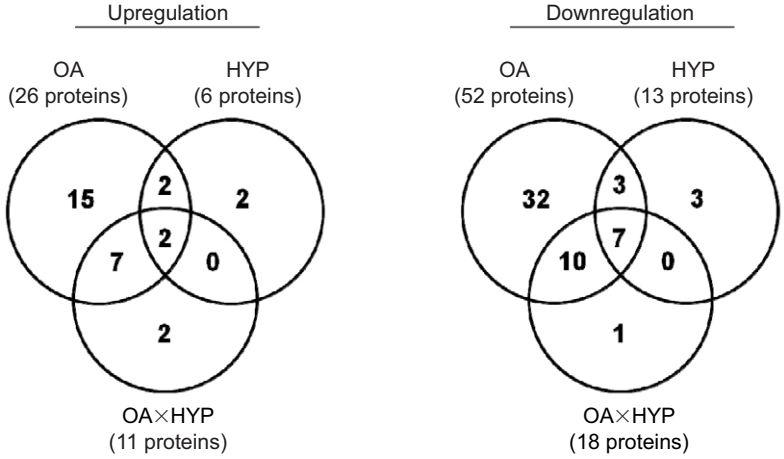

Fig. 6. Venn diagram showing the number of significantly upregulated or downregulated total proteins in the ocean acidification (OA), hypoxia (HYP) or combined OA×HYP groups compared with the control.

overexpressed (Sussarellu et al., 2010). Significantly, we found few commonalities in the proteome responses to the individual OA or HYP treatments compared with the combined treatment. We hypothesize that such a shift in the expression pattern could occur in two scenarios: (1) HYP could exert a compensatory effect on the expression of OA-altered proteins using an agonistic coordinated regulatory mechanism, or (2) the simultaneous exposure to the two stressors could have affected the ability of the juvenile tubeworm to perform precise cellular functions (in terms of protein expression).

Differential expression of proteins

The differential expression pattern of proteins in response to treatment conditions was analyzed using a volcano plot (Fig. 5) and a Venn diagram (Fig. 6). In the volcano plot, proteins outside the shaded area were either differentially upregulated or downregulated by the respective treatments. In response to OA, several proteins were differentially expressed and were more downregulated compared with the control. Similar trends, although much less pronounced, were observed in the HYP and OA×HYP groups. More proteins were upregulated in response to OA×HYP compared with the OA group. In the Venn diagram, out of 26 proteins elevated in the OA group, only four of them overlapped with those in the HYP group. Similarly, only 10 proteins overlapped out of the 52 and 13 downregulated proteins in OA and HYP groups, respectively. Around four times as many proteins appeared to be regulated by the tubeworms in the OA than in the HYP groups. This indicates that the OA stress alone could pose a greater threat to the tubeworms than HYP stress alone. Notably, 11 proteins were upregulated and 18 proteins were downregulated in the OA×HYP group.

These findings were in agreement with the PCA analysis (Fig. 4). Taken together, the results imply that OA may have a greater influence on the tubeworms than the other treatments, as seen by the comparatively greater number and magnitude of expression changes, and when combined (OA×HYP), hypoxia seemed to compensate for or counteract the negative effects of OA. The overall expression pattern was comparatively ‘normal’, resembling more the control expression pattern. The proteome response in the combined OA×HYP group was relatively distinct from the response in the individual stressor groups. The quantitative analysis of expressed total proteins identified 13 differentially expressed protein spots among the different treatment conditions (Table 1). All the identified and differentially expressed spots had a ≥1.5-fold increase in abundance in response to OA, HYP or OA×HYP compared with controls (Fig. 7). These proteins were classified into different functional groups (Fig. 8) and their potential roles in tubeworm tolerance to OA and/or HYP were then inferred. As with many

Table 1. List of larval proteins that were differentially expressed in response to climate change conditions [ocean acidification (OA), hypoxia (HYP) and OA×HYP] and subsequently identified using MALDI-TOF/TOF MS/MS and DeNovo sequencing analysis

Assigned spot no.	Fold change			*P*	Putative protein identification	MASCOT protein score (CI)	DeNovo Explorer score
	OA	HYP	OA×HYP				
a	↓ 6.70	↓ 3.16	↓ 3.46	0.002	ATP synthase beta subunit	336 (100)	
b	↓ 1.92	↓ 1.05	↑ 1.03	0.001	Calretuculin	93 (99.95)	
c	↓ 2.52	↓ 1.42	↓ 1.79	0.025	SCBP3 protein	111 (100)	
d	↓ 2.06	↓ 1.48	↓ 1.37	0.006	Putative tudor and KH domain containing protein	84 (99.65)	
e	↓ 3.17	↓ 1.86	↓ 2.10	0.009	ATP synthase beta subunit	279 (100)	
f	↓ 3.54	↓ 2.58	↓ 3.45	0.005	Chaperonin Hsp-60	157 (100)	
g	↑ 1.70	↑ 1.29	↑ 1.61	0.012	Calreticulin		81.2
h	↓ 3.95	↓ 1.44	↓ 1.41	<0.001	Protein disulfide-isomerase 2 precursor		61.4
i	↓ 3.11	↓ 1.50	↓ 2.14	0.004	14-3-3-like protein		78.9
j	↓ 10.5	↓ 1.98	↓ 2.50	0.001	Actin 5C	391 (100)	
k	↓ 2.34	↓ 1.42	↓ 1.73	0.038	Actin	393 (100)	
l	↓ 5.85	↓ 2.22	↓ 2.35	0.006	Alpha-tubulin	475 (100)	
m	↓ 2.62	↓ 1.03	↓ 1.39	<0.001	Putative tubulin, beta, 2	505 (100)	

Sample spot number refers to numbered spots in the 2-DE images shown in Fig. 2.

Fold-change values are expressed relative to controls.

The in-house MASCOT protein score (presented with 95% confidence intervals) was obtained by searching against the NCBI non-redundant database and taxonomy as ‘other Metazoa’. A MASCOT score >50 was considered significant.

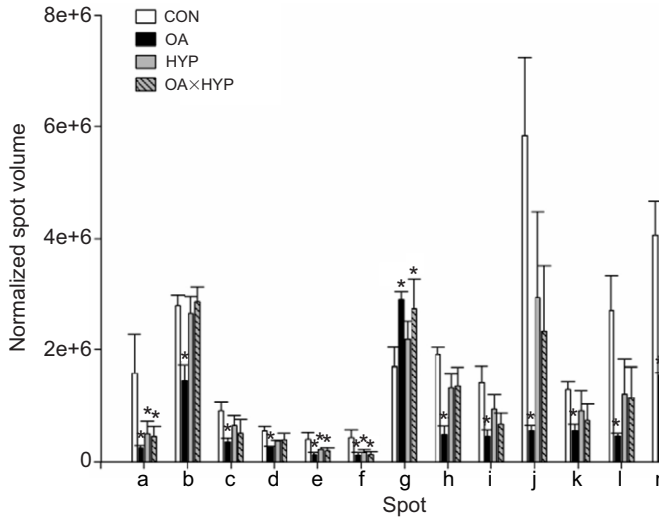

Fig. 7. Fold changes of the 13 differentially expressed total proteins in the ocean acidification (OA), hypoxia (HYP) or combined OA×HYP groups compared with the control (CON). A change was defined as a ≥1.5-fold difference in abundance, and statistical significance was set at $P<0.05$.

proteomics studies in non-model species, the expression data obtained from this study are largely exploratory.

Cytoskeletal proteins

Cytoskeletal protein isoforms constitute their own group among the differentially expressed proteins. The two isoforms of actin and tubulin were downregulated in all of the treatments (actin, spots j and k; tubulin, spots l and m). Remarkably, one actin isoform (spot j) showed a greater than 10-fold repression under OA. Such a major downregulation may be linked to metamorphosis, where resorption of the preceding larval structures occurs (Hadfield, 2000). Furthermore, structural proteins are generally prominent targets in multiple taxa response to stress. These include the isoforms of actin and tubulin, which are 'universal' cellular stress response proteins. Structural proteins are regarded as key regulators of many cellular processes, ranging from proper cell division to maintaining cell shape and cytoskeletal remodeling (Hammond et al., 2008). It would be reasonable to suggest that structural protein isoforms can change their expression in response to climate change. Several new studies shed light on the regulation of cytoskeletal dynamics in the response of marine taxa to OA and/or HYP. For example, beta-tubulin was downregulated in oyster larvae reared under OA (Dineshram et al., 2012). In contrast, several actin isoforms were upregulated under OA in the mantle tissue of adult oysters (Tomanek et al., 2011). Similarly, differential cytoskeletal protein regulation was reported in a proteome investigation of Chinese shrimp in response to HYP (Jiang et al., 2009). Given the general importance and ubiquitous nature of structural proteins, we confirmed the expression level of tubulin by western blotting (Fig. 9). Tubulin was the only immunologically confirmed protein in the present study because of the limited availability of antibodies that show good reactivity in tubeworms. Tubulin was detected as a band around 50 kDa in the control sample. Differential regulation was consistent under all the climate change conditions. The western blots were validated using actin as the positive control (Chandramouli et al., 2012; Zhang et al., 2010a).

Calcification-related proteins

We observed two isoforms of a calcium binding protein, calreticulin, which displayed an opposite pattern of change across treatments. One calreticulin isoform (spot b) was specifically downregulated twofold under OA. Similarly, a soluble calcium binding protein (SCBP3; spot c) was downregulated 2.5-fold under OA (Fig. 7). Calreticulin is a conserved endoplasmic reticulum protein that is essential to and expressed in all eukaryotic organisms (Jia et al., 2009). This protein plays key roles in diverse cellular processes such as molecular chaperone/protein folding and calcium-related metabolism (Michalak et al., 2002). Recent studies on molluscs indicate that calreticulin plays a significant role in shell formation (e.g. Fan et al., 2008). Similar roles have been demonstrated in apple snail development and shell formation (Sun et al., 2010). It is thus tempting to speculate that the observed regulation in calreticulin isoforms, together with SCBP3, would exert a selective change in the calcium homeostasis and hence affect the calcification machinery of the tubeworms. Recent studies have shown that elevated levels of calcification-related genes could translate into greater tolerance of $CaCO_3$ structures to OA in urchin larvae (Martin et al., 2011), corals (Reyes-Bermudez et al., 2009) and oysters (Dineshram et al., 2012). Our observation that calreticulin was downregulated in OA could reflect the newly metamorphosed larva's early response to the 'hostile' effects on shell formation in climate-change-related OA. In contrast, downregulation of calreticulin could also be associated with a compromise in juvenile's tolerance to climate change in the benthic environment.

In contrast to the OA treatment, calreticulin (spot b in Table 1) was significantly upregulated in OA×HYP, which was consistent with our observation that *H. elegans* was able to carry out calcification even when exposed to both stressors. The sustained expression of the calreticulin could be due to the compensatory effect of HYP on OA, restoring the protein expression to a level similar to the control level. When faced the combined stressors, tubeworms seem to be able to tolerate or compensate for adverse changes in environments to maintain normal physiological functions, preferably *via* a plastic proteome response.

Metabolism-related proteins

The expression of two isoforms of the mitochondrial precursor of ATP synthase beta-subunit were downregulated by all treatments

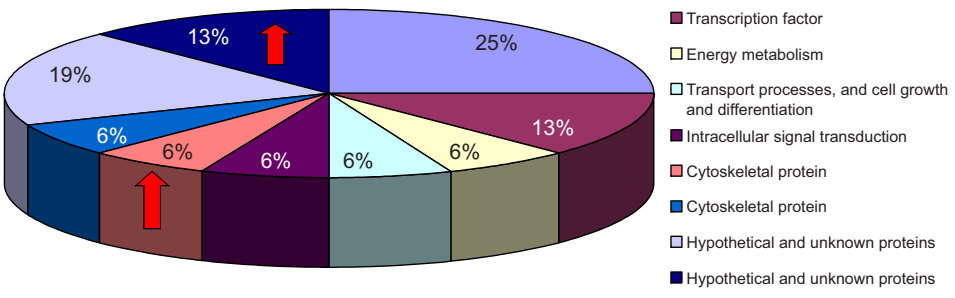

Fig. 8. Functional groups of the differentially expressed proteins in the control (CON), ocean acidification (OA), hypoxia (HYP) and combined OA×HYP groups are represented as percentages in the pie chart. The two arrows represent upregulation and the rest are downregulation.

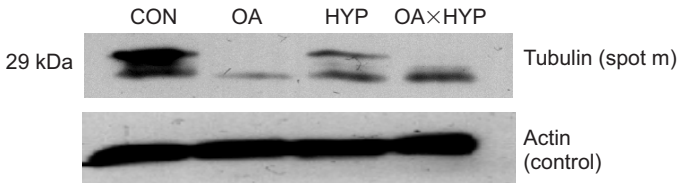

Fig. 9. Representative image of the 1-D gel and western blot analysis of tubulin and actin of newly metamorphosed *Hydroides elegans* larvae probed with anti-tubulin and anti-actin monoclonal antibodies using electrochemiluminescence. Samples are from the control (CON), ocean acidification (OA), hypoxia (HYP) and combined OA×HYP groups.

(spots a and e), with the greatest changes in the OA group (Fig. 7). Mitochondrial ATP synthases are key metabolic enzymes that manufacture ATP, the universal energy currency of cells (Walker et al., 1982). Therefore, a disruption to ATP production would result in decreased metamorphosis (Fig. 1), as seen by a lower percentage of metamorphosed larvae under OA compared with other conditions within the experimental period. The downregulation of mitochondrial ATP synthase beta-subunit protein in the HYP and OA×HYP groups was less compared with that of the OA group, implying less stress to metamorphosing larvae under these conditions compared with OA. In spite of the potentially 'adaptive/acclimatory' suppression in metabolism, we cannot preclude the possibility that a mode-of-action by OA, HYP and combined OA×HYP could involve perturbations in ATP synthesis and mitochondrial metabolism. This cause-and-effect relationship needs to be addressed in future research.

Conclusions

This study sheds light on proteome changes underlying the acclimatory response of newly metamorphosed larvae to climate change. Exposure to multiple climate change stressors caused several proteins involved in energy metabolism, calcification and stress tolerance to be differentially expressed, which seemed to allow the tubeworm larvae to successfully metamorphose and carry out calcification. Our results suggest that the aragonite tube-forming tubeworm larvae have a high tolerance to hypoxia and may possess the capacity to acclimate over time, even in the phase of ocean acidification. Further, this study demonstrated the usefulness of a 2-DE-based proteomic approach to explore the short-term adaptive or acclimatory responses of a non-model marine invertebrate species to climate change stressors.

ACKNOWLEDGEMENTS

We thank Gray Williams and Kenneth Leung (University of Hong Kong) and Jill Chiu (Hong Kong Baptist University) for their valuable discussions during the course of this project and for their support in setting up the ocean acidification and hypoxia facilities in our laboratory. We also thank Fariba Babaei of the City University of Hong Kong for her help with the volcano plot.

AUTHOR CONTRIBUTIONS

J.M. and K.K.W.W.: conception, design and execution; K.H.C. and P.-Y.Q.: interpretation of findings; P.T.Y.L. and R.S.S.W.: revising the article; V.T.: drafting and revising the article. J.M. and K.K.W.W. contributed equally to this work.

COMPETING INTERESTS

No competing interests declared.

FUNDING

This study was supported by a grant from the Area of Excellency Project (no. AoE/P-04/2004) and Hong Kong Research Grants Council research funds (nos 778309M and 764711M).

REFERENCES

Byrne, M. (2011). Impact of ocean warming and ocean acidification on marine invertebrate life history stages: vulnerabilities and potential for persistence in a changing ocean. *Oceanogr. Mar. Biol. Annu. Rev.* **49**, 1-42.

Caldeira, K. and Wickett, M. E. (2005). Ocean model predictions of chemistry changes from carbon dioxide emissions to the atmosphere and ocean. *J. Geophys. Res.* **110**, C09S04.

Candiano, G., Bruschi, M., Musante, L., Santucci, L., Ghiggeri, G. M., Carnemolla, B., Orecchia, P., Zardi, L. and Righetti, P. G. (2004). Blue silver: a very sensitive colloidal Coomassie G-250 staining for proteome analysis. *Electrophoresis* **25**, 1327-1333.

Carpentier, S. C., Panis, B., Vertommen, A., Swennen, R., Sergeant, K., Renaut, J., Laukens, K., Witters, E., Samyn, B. and Devreese, B. (2008). Proteome analysis of non-model plants: a challenging but powerful approach. *Mass Spectrom. Rev.* **27**, 354-377.

Chan, V. B. S., Li, C., Lane, A. C., Wang, Y., Lu, X., Shih, K., Zhang, T. and Thiyagarajan, V. (2012). CO_2-driven ocean acidification alters and weakens integrity of the calcareous tubes produced by the serpulid tubeworm, *Hydroides elegans*. *PLoS ONE* **7**, e42718.

Chandramouli, K. H., Mok, F. S., Wang, H. and Qian, P. Y. (2011). Phosphoproteome analysis during larval development and metamorphosis in the spionid polychaete *Pseudopolydora vexillosa*. *BMC Dev. Biol.* **11**, 31.

Chandramouli, K. H., Zhang, Y., Wong, Y. H. and Qian, P. Y. (2012). Comparative glycoproteome analysis: dynamics of protein glycosylation during metamorphic transition from pelagic to benthic life stages in three invertebrates. *J. Proteome Res.* **11**, 1330-1340.

Diaz, R. J. and Rosenberg, R. (1995). Marine benthic hypoxia: a review of its ecological effects and the behavioural responses of benthic macrofauna. *Oceanogr. Mar. Biol. Annu. Rev.* **33**, 245-303.

Dineshram, R., Wong, K. K., Xiao, S., Yu, Z., Qian, P. Y. and Thiyagarajan, V. (2012). Analysis of Pacific oyster larval proteome and its response to high-CO_2. *Mar. Pollut. Bull.* **64**, 2160-2167.

Dineshram, R., Thiyagarajan, V., Lane, A., Ziniu, Y., Xiao, S. and Leung, P. Y. (2013). Elevated CO_2 alters larval proteome and its phosphorylation status in the commercial oyster, *Crassostrea hongkongensis*. *Mar. Biol.* **160**, 2189-2205.

Diz, A. P. and Skibinski, D. O. F. (2007). Evolution of 2-DE protein patterns in a mussel hybrid zone. *Proteomics* **7**, 2111-2120.

Dreanno, C., Matsumura, K., Dohmae, N., Takio, K., Hirota, H., Kirby, R. R. and Clare, A. S. (2006). An α2-macroglobulin-like protein is the cue to gregarious settlement of the barnacle *Balanus amphitrite*. *Proc. Natl. Acad. Sci. USA* **103**, 14396-14401.

Dupont, S. and Thorndyke, M. C. (2009). Impact of CO_2-driven ocean acidification on invertebrates' early life-history: what we know, what we need to know and what we can do. *Biogeosciences* **6**, 3109-3131.

Ekau, W., Auel, H., Pörtner, H. O. and Gilbert, D. (2010). Impacts of hypoxia on the structure and processes in pelagic communities (zooplankton, macro-invertebrates and fish). *Biogeosciences* **7**, 1669-1699.

Fabry, V. J., Seibel, B. A., Feely, R. A. and Orr, J. C. (2008). Impacts of ocean acidification on marine fauna and ecosystem processes. *ICES J. Mar. Sci.* **65**, 414-432.

Fan, W., Hu, Y., Li, C., Xie, L. and Zhang, R. (2008). Cloning, characterization, and expression analysis of calreticulin from Pearl oyster *Pinctada fucata*. *Tsinghua Sci. Technol.* **13**, 466-473.

Feely, R. A., Sabine, C. L., Lee, K., Berelson, W., Kleypas, J., Fabry, V. J. and Millero, F. J. (2004). Impact of anthropogenic CO_2 on the $CaCO_3$ system in the oceans. *Science* **305**, 362-366.

Gilbert, D., Rabalais, N. N., Díaz, R. J. and Zhang, J. (2010). Evidence for greater oxygen decline rates in the coastal ocean than in the open ocean. *Biogeosciences*, **7**, 2283-2296.

Hadfield, M. G. (2000). Why and how marine invertebrate larvae metamorphose so fast. *Semin. Cell Dev. Biol.* **11**, 437-443.

Hadfield, M. G. (2011). Biofilms and marine invertebrate larvae: what bacteria produce that larvae use to choose settlement sites. *Ann. Rev. Mar. Sci.* **3**, 453-470.

Halko, N., Martinsson, P.-G., Shkolnisky, Y. and Tygert, M. (2011). An algorithm for the principal component analysis of large data sets. *SIAM J. Sci. Comput.* **33**, 2580-2594.

Hammond, J. W., Cai, D. and Verhey, K. J. (2008). Tubulin modifications and their cellular functions. *Curr. Opin. Cell Biol.* **20**, 71-76.

Hayward, D. C., Hetherington, S., Behm, C. A., Grasso, L. C., Forêt, S., Miller, D. J. and Ball, E. E. (2011). Differential gene expression at coral settlement and metamorphosis – a subtractive hybridization study. *PLoS ONE* **6**, e26411.

Hofmann, G. E., Barry, J. P., Edmunds, P. J., Gates, R. D., Hutchins, D. A., Klinger, T. and Sewell, M. A. (2010). The effect of ocean acidification on calcifying organisms in marine ecosystems: an organism-to-ecosystem perspective. *Annu. Rev. Ecol. Syst.* **41**, 127-147.

Howarth, R., Chan, F., Conley, D. J., Garnier, J., Doney, S. C., Marino, R. and Billen, G. (2011). Coupled biogeochemical cycles: eutrophication and hypoxia in temperate estuaries and coastal marine ecosystems. *Front. Ecol. Environ* **9**, 18-26.

Huang, Y., Callahan, S. and Hadfield, M. G. (2012). Recruitment in the sea: bacterial genes required for inducing larval settlement in a polychaete worm. *Scientific Reports* **2**, 228.

Jia, X.-Y., He, L.-H., Jing, R.-L. and Li, R. Z. (2009). Calreticulin: conserved protein and diverse functions in plants. *Physiol. Plant.* **136**, 127-138.

Jiang, H., Li, F., Xie, Y., Huang, B., Zhang, J., Zhang, J., Zhang, C., Li, S. and Xiang, J. (2009). Comparative proteomic profiles of the hepatopancreas in *Fenneropenaeus chinensis* response to hypoxic stress. *Proteomics* **9**, 3353-3367.

Lane, A. C., Mukherjee, J., Chan, V. B. S. and Thiyagarajan, V. (2013). Decreased pH does not alter metamorphosis but compromises juvenile calcification of the tube worm *Hydroides elegans*. *Mar. Biol.* **63**, 1983-1993.

Leung, Y., Shin, P., Qiu, J., Ang, P., Chiu, J., Thiyagarajan, V. and Cheung, S. (2013). Physiological and behavioural responses of different life stages of a serpulid polychaete to hypoxia. *Mar. Ecol. Prog. Ser.* **477**, 135-145.

Lewis, E. and Wallace, D. W. R. (1998). Program developed for CO_2 system calculations. ORNL/CDIAC-105. Oak Ridge, TN: Carbon Dioxide Information Analysis Center, Oak Ridge National Laboratory, United States Department of Energy.

Lindgren, J. F., Haeffner, M., Ericsson, C. T. and Jonsson, P. R. (2009). Oxygen-depleted surfaces: a new antifouling technology. *Biofouling* **25**, 455-461.

Lo, K. H., Hui, M. N. Y., Yu, R. M. K., Wu, R. S. S. and Cheng, S. H. (2011). Hypoxia impairs primordial germ cell migration in zebrafish (*Danio rerio*) embryos. *PLoS ONE* **6**, e24540.

Martin, S., Richier, S., Pedrotti, M. L., Dupont, S., Castejon, C., Gerakis, Y., Kerros, M.-E., Oberhänsli, F., Teyssié, J. L., Jeffree, R. et al. (2011). Early development and molecular plasticity in the Mediterranean sea urchin *Paracentrotus lividus* exposed to CO_2-driven acidification. *J. Exp. Biol.* **214**, 1357-1368.

McDonagh, B. and Sheehan, D. (2006). Redox proteomics in the blue mussel *Mytilus edulis*: carbonylation is not a pre-requisite for ubiquitination in acute free radical-mediated oxidative stress. *Aquat. Toxicol.* **79**, 325-333.

Melzner, F., Thomsen, J., Koeve, W., Oschlies, A., Gutowska, M., Bange, H., Hansen, H. and Körtzinger, A. (2013). Future ocean acidification will be amplified by hypoxia in coastal habitats. *Mar. Biol.* **160**, 1875-1888.

Michalak, M., Robert Parker, J. M. and Opas, M. (2002). Ca^{2+} signaling and calcium binding chaperones of the endoplasmic reticulum. *Cell Calcium* **32**, 269-278.

Mok, F. S., Thiyagarajan, V. and Qian, P. Y. (2009). Proteomic analysis during larval development and metamorphosis of the spionid polychaete *Pseudopolydora vexillosa*. *Proteome Sci.* **7**, 44.

Nedved, B. T. and Hadfield, M. G. (2009). *Hydroides elegans* (Annelida: Polychaeta): a model for biofouling research. In *Marine and Industrial Biofouling*, Vol. 4 (ed. H.-C. Flemming, P. S. Murthy, R. Venkatesan and K. Cooksey), pp. 203-217. Berlin: Springer.

Nunn, B. L. and Timperman, A. T. (2007). Marine proteomics. *Mar. Ecol. Prog. Ser.* **332**, 281-289.

Pechenik, J. A. and Qian, P. Y. (1998). Onset and maintenance of metamorphic competence in the marine polychaete *Hydroides elegans* Haswell in response to three chemical cues. *J. Exp. Mar. Biol. Ecol.* **226**, 51-74.

Pechenik, J. A., Pearse, J. S. and Qian, P. Y. (2007). Effects of salinity on spawning and early development of the tube-building polychaete *Hydroides elegans* in Hong Kong: not just the sperm's fault? *Biol. Bull.* **212**, 151-160.

Peña, M. A., Katsev, S., Oguz, T. and Gilbert, D. (2010). Modeling dissolved oxygen dynamics and hypoxia. *Biogeosciences* **7**, 933-957.

Pörtner, H. O. (2008). Ecosystem effects of ocean acidification in times of ocean warming: a physiologist's view. *Mar. Ecol. Prog. Ser.* **373**, 203-217.

Qian, P. Y. (1999). Larval settlement of polychaetes. *Hydrobiologia* **402**, 239-253.

Qian, P. Y. and Pechenik, J. A. (1998). Effects of larval starvation and delayed metamorphosis on juvenile survival and growth of the tube-dwelling polychaete *Hydroides elegans* (Haswell). *J. Exp. Mar. Biol. Ecol.* **227**, 169-185.

Rabalais, N. N., Díaz, R. J., Levin, L. A., Turner, R. E., Gilbert, D. and Zhang, J. (2010). Dynamics and distribution of natural and human-caused hypoxia. *Biogeosciences* **7**, 585-619.

Ramagli, L. S. (1999). Quantifying protein in 2-D PAGE solubilization buffers. *Methods Mol. Biol.* **112**, 99-103.

Reyes-Bermudez, A., Desalvo, M. K., Voolstra, C. R., Sunagawa, S., Szmant, A. M., Iglesias-Prieto, R. and Medina, M. (2009). Gene expression microarray analysis encompassing metamorphosis and the onset of calcification in the scleractinian coral *Montastraea faveolata*. *Mar. Genomics* **2**, 149-159.

Riebesell, U., Fabry, V. J., Hanson, L. and Gattuso, J.-P. (2010). *Guide to Best Practices For Ocean Acidification Research and Data Reporting*. Luxembourg: Publications Office of the European Union.

Sabine, C. L., Feely, R. A., Gruber, N., Key, R. M., Lee, K., Bullister, J. L., Wanninkhof, R., Wong, C. S., Wallace, D. W. R., Tilbrook, B. et al. (2004). The oceanic sink for anthropogenic CO_2. *Science* **305**, 367-371.

Seibel, B. A. (2011). Critical oxygen levels and metabolic suppression in oceanic oxygen minimum zones. *J. Exp. Biol.* **214**, 326-336.

Shevchenko, A., Tomas, H., Havlis, J., Olsen, J. V. and Mann, M. (2007). In-gel digestion for mass spectrometric characterization of proteins and proteomes. *Nat. Protoc.* **1**, 2856-2860.

Sun, J., Zhang, Y., Thiyagarajan, V., Qian, P. Y. and Qiu, J. W. (2010). Protein expression during the embryonic development of a gastropod. *Proteomics* **10**, 2701-2711.

Sunday, J. M., Crim, R. N., Harley, C. D. G. and Hart, M. W. (2011). Quantifying rates of evolutionary adaptation in response to ocean acidification. *PLoS ONE* **6**, e22881.

Sussarellu, R., Fabioux, C., Le Moullac, G., Fleury, E. and Moraga, D. (2010). Transcriptomic response of the Pacific oyster *Crassostrea gigas* to hypoxia. *Mar. Genomics* **3**, 133-143.

Talmage, S. C. and Gobler, C. J. (2011). Effects of elevated temperature and carbon dioxide on the growth and survival of larvae and juveniles of three species of northwest Atlantic bivalves. *PLoS ONE* **6**, e26941.

Thiyagarajan, V. (2010). A review on the role of chemical cues in habitat selection by barnacles: new insights from larval proteomics. *J. Exp. Mar. Biol. Ecol.* **392**, 22-36.

Thiyagarajan, V. and Qian, P. Y. (2008). Proteomic analysis of larvae during development, attachment, and metamorphosis in the fouling barnacle, *Balanus amphitrite*. *Proteomics* **8**, 3164-3172.

Thiyagarajan, V., Wong, T. and Qian, P. Y. (2009). 2D gel-based proteome and phosphoproteome analysis during larval metamorphosis in two major marine biofouling invertebrates. *J. Proteome Res.* **8**, 2708-2719.

Tomanek, L. (2006). Pitfall or promise: proteomics for non-model organisms. *J. Exp. Biol.* **209**, vi.

Tomanek, L. (2011). Environmental proteomics: changes in the proteome of marine organisms in response to environmental stress, pollutants, infection, symbiosis, and development. *Ann. Rev. Mar. Sci.* **3**, 373-399.

Tomanek, L., Zuzow, M. J., Ivanina, A. V., Beniash, E. and Sokolova, I. M. (2011). Proteomic response to elevated P_{CO_2} level in eastern oysters, *Crassostrea virginica*: evidence for oxidative stress. *J. Exp. Biol.* **214**, 1836-1844.

Vinn, O., tenHove, H. A. and Mutvei, H. (2008). On the tube ultrastructure and origin of calcification in sabellids (Annelida, Polychaeta). *Palaeontology* **51**, 295-301.

Walker, J. E., Saraste, M., Runswick, M. J. and Gay, N. J. (1982). Distantly related sequences in the alpha- and beta-subunits of ATP synthase, myosin, kinases and other ATP-requiring enzymes and a common nucleotide binding fold. *EMBO J.* **1**, 945-951.

Wong, K. K. W., Lane, A. C., Leung, P. T. Y. and Thiyagarajan, V. (2011). Response of larval barnacle proteome to CO_2-driven seawater acidification. *Comp. Biochem. Physiol.* **6D**, 310-321.

Wu, R. S. S. (2009). Effects of hypoxia on fish reproduction and development. In *Fish Physiology*, Chapter 3, Vol. 27 (ed. A. P. F. Jeffrey, G. Richards and J. B. Colin), pp. 79-141. Academic Press.

Yang, Y., Wang, J., Bu, D., Zhang, L., Li, S., Zhou, L. and Wei, H. (2011). A fluorescence-based Coomassie Blue protocol for two-dimensional gel-based proteomics. *Biotechnol. Lett.* **33**, 119-121.

Zhang, Y., Sun, J., Xiao, K., Arellano, S. M., Thiyagarajan, V. and Qian, P. Y. (2010a). 2D gel-based multiplexed proteomic analysis during larval development and metamorphosis of the biofouling polychaete tubeworm *Hydroides elegans*. *J. Proteome Res.* **9**, 4851-4860.

Zhang, Y., Xu, Y., Arellano, S. M., Xiao, K. and Qian, P. Y. (2010b). Comparative proteome and phosphoproteome analyses during cyprid development of the barnacle *Balanus* (=*Amphibalanus*) *amphitrite*. *J. Proteome Res.* **9**, 3146-3157.